Research Article

Bulk Heterojunction Solar Cell Devices Prepared with Composites of Conjugated Polymer and Zinc Oxide Nanorods

Nguyen Tam Nguyen Truong, Hoa Nguyen, Phuc Huu Tran Le, Chinho Park, and Jae Hak Jung

School of Chemical Engineering, Yeungnam University, 280 Daehak-Ro, Gyeongsan 712-749, Republic of Korea

Correspondence should be addressed to Chinho Park; chpark@ynu.ac.kr and Jae Hak Jung; jhjung@ynu.ac.kr

ZnO nanorods (Nrods) with ~20–50 nm lengths were synthesized using an aqueous solution of zinc acetate and glacial acetic acid. Bulk heterojunction solar cells were fabricated with the structure of indium tin oxide (ITO)/polyethylenedioxythiophene doped with polystyrene-sulfonic acid (PEDOT:PSS)/ZnO-Nrods + polymer/electron transport layer (ETL)/Al. Current density-voltage characterization of the resulting cells showed that, by adding an ETL and using polymers with a low band gap energy, the photoactive layer surface morphology and the device performance can be dramatically improved.

1. Introduction

Semiconducting inorganic nanocrystals (NCs) with different shapes such as nanowires, nanospheres, nanosheets, nanotetrapods, and nanorods have attracted significant attention in the field of materials science owing to their promising applications in optoelectronic devices such as inorganic and organic light emitting diodes and photovoltaic devices [1–3]. The first hybrid photovoltaic device using CdS and CdSe NCs was reported by Greenham et al. [4]. Since then, inorganic semiconducting NCs, such as PbS, CdS, and CdSe NCs, with different structures, sizes, shapes, and morphological characteristics have been investigated and applied for hybrid bulk heterojunction (BHJ) photovoltaic devices [5–7]. However, note that the above materials, including cadmium, lead, and indium, are either nonabundant or toxic, so these materials cannot contribute significantly to future green, eco-friendly technologies and renewable energy. Therefore, low-cost, non-toxic, and eco-friendly semiconducting materials are being extensively explored as alternatives to existing materials for hybrid solar cells, even though they might produce lower power conversion efficiencies. Metal oxide nanostructures in particular have attracted considerable attention for their potential applications, for example, in solar cells, electroluminescent devices, electrochromic windows, and chemical sensors [8–11]. The metal oxide nanostructures used in these applications must have a large surface area and good photoelectronic, electrochemical, and structural properties.

ZnO is a wide-band-gap semiconductor with an energy gap of 3.37 eV at room temperature. Many different ZnO structures have been investigated for solar cell applications [12–14]. Since ZnO shows different chemical and physical properties depending on the size and shape of NCs, it might easily form a penetration network between particles; this is greatly beneficial for charge carrier transportation.

Hybrid polymer-ZnO NCs have been studied [15, 16], and ZnO NCs have been investigated as the n-type material in cells as they are cheap and eco-friendly and can be synthesized with high purity and crystallinity at low temperatures. However, results show that the device efficiency in these previous papers was lower (efficiency ~ 1.6%) than that of other hybrid BHJ solar cells because of unoptimized photoactive surface morphology, light absorption, and charge transport (collect) efficiency.

In order to enhance the device efficiency, the effects of various processing conditions, such as the absorption

coefficient of the materials, the thickness of the photoactive layer, and the charge carrier transports, were studied. The active layer should absorb as many photons as possible to generate the electron-hole pairs. Therefore, the thickness and surface morphology of the active layer should be well controlled and optimized. The contact should collect as many charge carriers as possible from the p-n junction. Therefore, the hole transport layer (HTL) and electron transport layer (ETL) should be added and optimized.

Conducting polymers such as poly(2-methoxy-5-($3'$,$7'$-dimethyloctyloxy)-1,4-phenylenevinylene) (MDMO PPV) and poly(3-hexylthiophene-2,5-diyl)(P3HT) have been employed in devices [17]. However, these polymers have a large band gap (from ~2 to 2.8 eV), which prevents the light absorption in the red region and near-IR region of the solar spectrum. Radiation with a long wavelength (>700 nm) passes through the diodes and makes a small contribution to the photocurrent. Therefore, new polymers with a low band gap of 1.3–1.4 eV (such as PCPDBTB and PTB7) were investigated; polymers with low band gap energy enable absorption of more photons with a long-wavelength spectrum.

In this study, high-quality and pure ZnO nanorods (Nrods) were synthesized and characterized for hybrid BHJ solar cell applications. Devices based on a blend of polymer and ZnO-Nrod NPs were fabricated. The device parameters including length of ZnO nanorods, absorption, and active layer surface morphology were investigated and characterized. The BHJ device based on a high-light-absorption polymer and ZnO nanorods exhibited extended red light harvesting up to 900 nm, in contrast to the typical 350–800 nm absorption in the case of P3HT and PCPDTBT. The improved BHJ device presents the possibility of fabricating low-cost, nontoxic, and eco-friendly inorganic/organic hybrid BHJ solar cells.

2. Experimental

In the typical procedure, 300 mL of 0.02 M zinc acetate aqueous solution was mixed with 1 mL glacial acetic acid in a round-bottomed flask equipped with a refluxing device. The solution was heated to 100°C with vigorous stirring, and then, about 0.8 g of NaOH solid (analytical grade, platelets) was rapidly added to the above boiling solution until the pH value of the mixture reached 6-7, at which point, a large amount of white precipitate was produced. After cooling to room temperature, the precipitate was centrifuged, washed once with distilled water and three times with absolute ethanol, and dried in air at 60°C. The resulting ZnO-Nrods were ~20–50 nm in length.

UV-Vis-NIR spectrophotometry (Cary 5000, Varian) over 200–800 nm, X-ray diffraction (XRD), and transmission electron microscopy (TEM) were used to characterize the optical and structural properties of the ZnO nanorods. The UV-vis (Cary 5000) spectra of the ZnO nanorods were obtained using quartz cells with a 1.0 cm path length. The samples were prepared by dispersing the nanoparticles in ethanol before the measurements. The size and shape of the NCs were estimated from the high-resolution transmission electron microscopic (HR-TEM, H-7600) images. The

thickness of active layers was measured by using Alpha-Step D-500 Stylus Profiler. The current density-voltage (J-V) characteristics of the solar cells were examined under AM1.5G illumination using a solar simulator (Keithley 69911).

Devices having the structure of glass/ITO/PEDOT:PSS/ (ZnO-Nrod + polymer)/ETL/Al were then fabricated. A thin (~70 nm) layer of PEDOT:PSS as HTL was spin-coated at 4000 rpm for 30 s onto cleaned indium tin oxide- (ITO-) coated glass substrates and dried at 120°C for 20 min. The composite solution of ZnO-Nrods and polymers such as poly(3-hexylthiophene-2,5-diyl)(P3HT), poly[2,6-(4,4-bis(2-ethylhexyl)-4H-cyclopenta[2,1-b;3,4-b']-dithiophene)-alt-4,7-(2,1,3-benzothiadiazole)] [PCPDTBT], and (poly({4,8-bis[(2-ethylhexyl)oxy]benzo[1,2-b:4,5-b']dithiophene-2,6-diyl}{3-fluoro-2-[(2ethylhexyl)carbonyl] thieno [3,4-b]thiophenediyl}) [PTB7]) was dropped and spin-coated onto the preformed PEDOT:PSS layers. Then the samples were dried at 140°C for 30 min and a thin layer of ZnO nanoparticles as the HTL was spin-coated onto the top of active layer. Finally, a ~90 nm thick Al electrode layer was deposited on the films by thermal evaporation to complete the devices. Figure 1 shows the schematic diagram of devices fabricated in this study, along with the materials structure.

3. Results and Discussion

Figures 2(a) and 2(a) (inset) show HR-TEM and TEM images of the ZnO nanorods. Nanorods in the range of 10–15 nm in diameter and in range of 20–50 nm in length had been formed. The lattice fringes of nanorod are clearly visible and no disruption inside the nanorods was presented, indicating that the ZnO nanorods obtained in this work were of high quality. Figure 2(b) is the UV-vis absorption spectra of ZnO-Nrods dispersed in ethanol solution. It shows a strong absorption peak in the range of 300–400 nm and the peak was observed at the 369 nm.

Figure 2(c) shows the XRD diffraction pattern of ZnO nanorods and it can be observed that all peaks at 2θ values of 31.5, 34.3, 36.4, 47.5, 56.5, 62.8, 67.9, and 72.5 can be indexed to the (100), (002), (101), (102), (110), (103), (112), and (004) planes of zinc oxide nanorods, respectively. The position of several XRD peaks matched very well with the standard diffraction data (Joint Committee for Power Diffraction Set (JCPDS) database number 80-0075). The diffraction peaks are quite similar to those of a bulk ZnO with the hexagonal structure and the strongest peaks were (100), (002), and (101) for the randomly oriented direction samples.

The surface morphology and roughness of the ZnO/ P3HT photoactive layer having different concentration of ZnO-Nrods at the fixed composite loading amount of 5 mg/mL were studied by AFM. The ZnO-Nrod concentrations were varied from 0 to 90 wt%. The J-V characteristics of the devices were measured at AM1.5G conditions by using a solar simulator, and the resulting device parameters such as the short circuit current density (J_{sc}), open circuit voltage (V_{oc}), fill factor (FF), and power conversion efficiency (η) are compared in Figure 3(b). Interestingly, among the cells with the ZnO-Nrod/P3HT composites, the maximum power conversion efficiency was achieved for the cell with
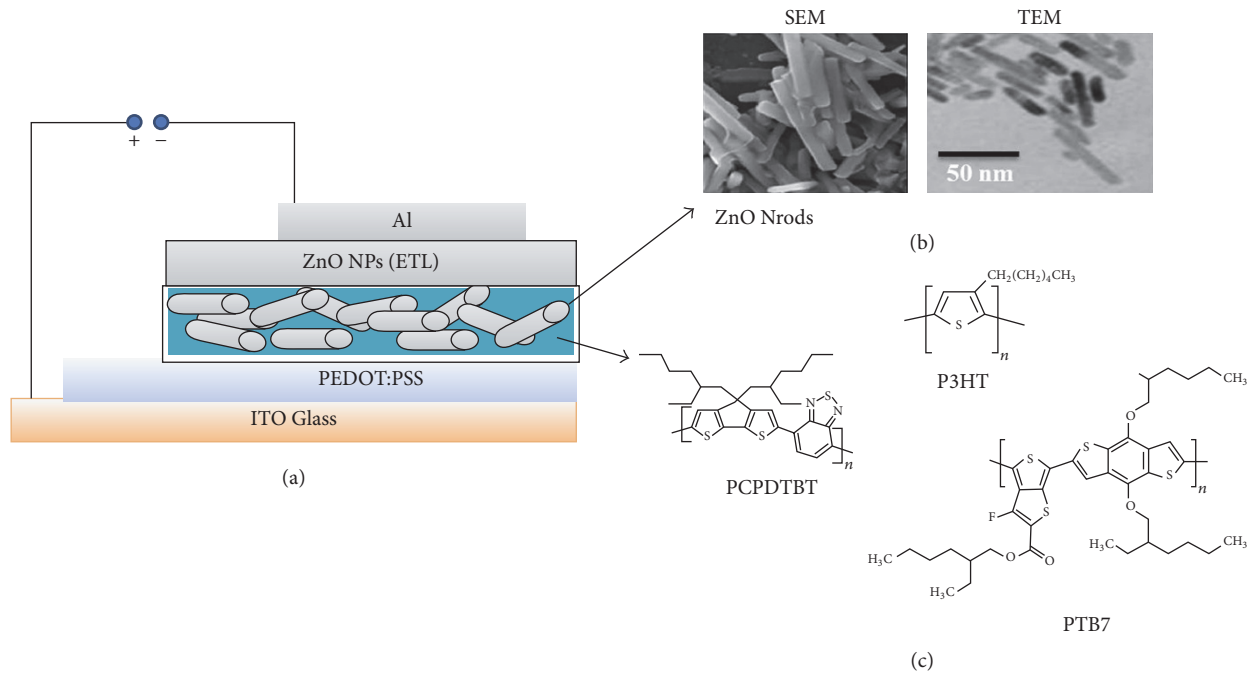
FIGURE 1: Schematic diagrams of (a) bulk heterojunction (BHJ) solar cells and (b) polymers and ZnO nanorods structure.

60 wt% ZnO-Nrods. This is consistent with the AFM surface roughness results, as shown in Figure 3(a).

Figure 3(b) (B and D) shows the monotonic increase in J_{sc} and efficiency with the increase in the ZnO/[ZnO + P3HT] (%) loading amount. It is confirmed that the increase in the Nrod concentration enhances the charge transport and collection efficiency by generating a larger photoactive interface area and reducing the carrier recombination rate; hence, the Nrods and P3HT polymer act as the electron and hole transport materials, respectively. Further, the fill factor and open circuit voltages likely remain unchanged until the Nrod concentration reached 60 wt% and then increased slightly. However, the results indicated that despite the slight increase in the device parameters as a function of the loading amount, their absolute values are still lower than the best reported values [15].

In case of standard and inverted device structures, the active layer materials have the same function with four main processes: (1) photon absorption from sunlight, (2) conversion of photons to free charge carriers, (3) transport of the electrons and holes to the contacts, and (4) extraction of these charge carriers at the contacts to generate useful power. In order to enhance the device performance, however, a BHJ should include both the HTL and ETL [18–20]. The overall reported power conversion efficiency using the HTL and ETL ranges from 2% to about 4%. In this study, the PEDOT:PSS (~70 nm thickness) was used as the HTL and the ZnO NPs deposition were selected as the ETL, as shown in Figure 1. One of the most important parameters that affect the device performance is the morphology (and, consequently, the surface roughness) of the ZnO layer. In this section, attention will be focused on the possible influences of the ETL layer surface morphology on device fabrication with various thicknesses.

TABLE 1: Electron transport layer's surface morphology as the junction of spin-speed of 1000, 2000, 3000, and 4000 round per minute.

ZnO (ETL) spin speed (rpm)	Roughness (RMS) (nm)	Contact angles (°)
1000	~5.92	~77.64
2000	~4.6	~56.64
3000	~3.91	~44.61
4000	~2.86	~38.61

Figure 4(a) shows the thickness of ZnO layer as the function of spin coating speed. The coating spin speed was varied in range of 1000 rounds per minute (rpm) to 4000 rpm. The figure shows that when the spin speed is increased, the ZnO thickness is decreased. At 4000 rpm, the ZnO film thickness is around ~30 nm. The effects of ZnO ETL on the morphology of the photoactive surface as a function of the spin speed were studied by AFM (roughness mean square (RMS)) and video contact angle measurement, as shown in Figure 4(b).

Figure 4(b), (A–D) and (E–K), shows the surface roughness (RMS) and the contact angle of photoactive layer as a function of the spin coating speed. We observed that when the speed is increased, the RMS and contact angle are decreased, as shown in Table 1. At the speed of 4000 rpm, the RMS and contact angle of the photoactive layer surface are 2.86 nm and 38.64°, respectively.

In particular, with the decrease in the thickness, the morphology of the ZnO ETL changed from a rough surface to a smoother surface to improve the contact between the photoactive layer and back contact layer.
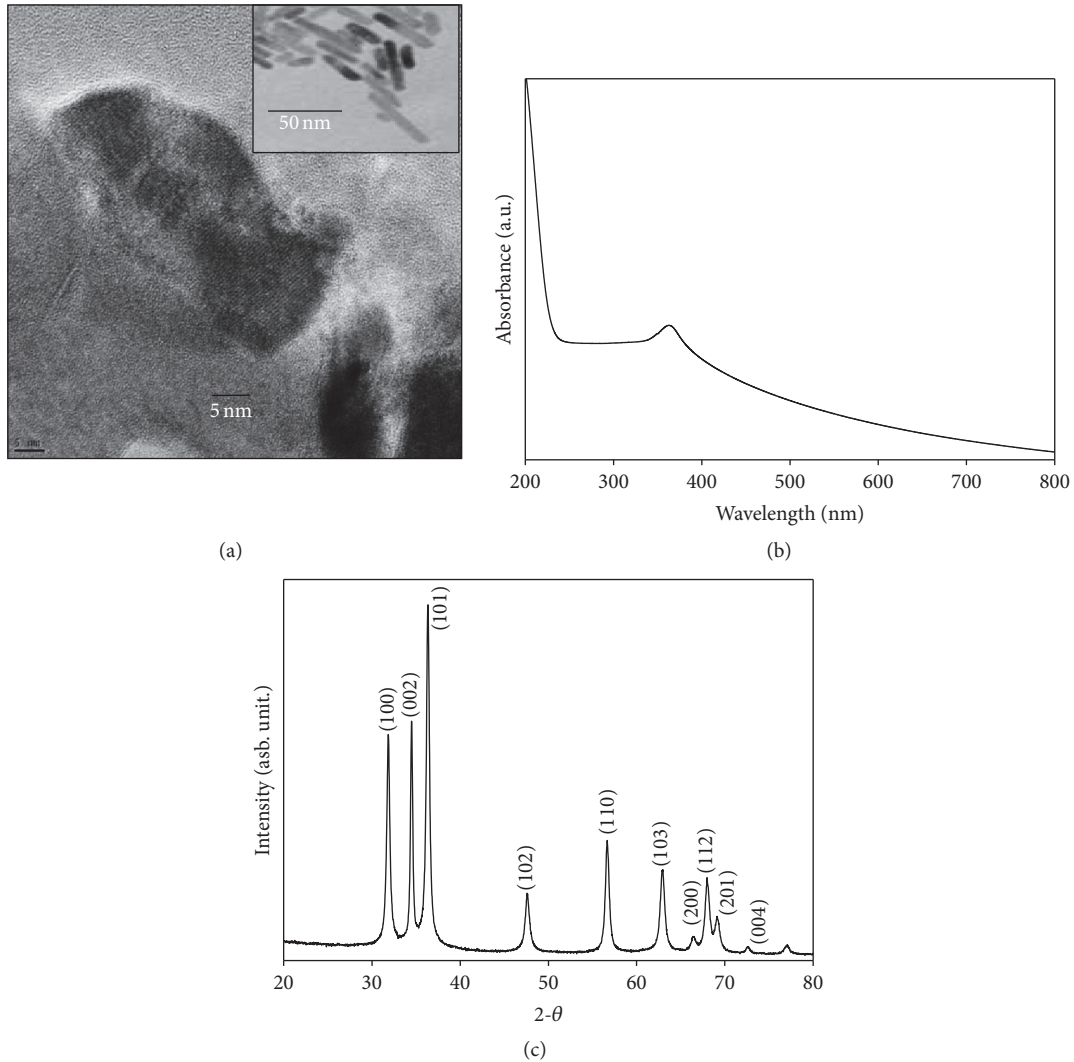
(a)

(b)

(c)

Figure 2: (a) High-resolution electron micrograph (HR-TEM) of single-crystal nanorods and (a) (inset) TEM image of ZnO nanorods; (b) UV-Vis absorption spectra of ZnO nanorods; (c) the XRD diffraction of the ZnO nanorods.

Figure 5 shows the effects of the ZnO layer (ETL) on the solar cell performance. In this study, ZnO nanoparticles were synthesized by laboratory, as shown in Figure 5 (inset). Figure 5 (inset (a)) shows the TEM image of ZnO NPs with a size of ~3–5 nm. Figure 5 (inset (b)) shows the ZnO NPs/ITO thin film (spin speed of 4000 rpm) with the surface roughness of ~2 nm. In a device without the ETL, the power conversion efficiency is about ~1.71% (J_{sc} ~ 8.64 mA/cm^2), but in a device with ZnO ETL, the efficiency is increased to ~2.25% (J_{sc} ~ 10.26 mA/cm^2); the detailed device parameters are shown in Table 2. The improvement in the device performance especially in the efficiency and current density might be attributed to the increase in the charge collection efficiency and to the reduction in the charge recombination from the p-n photoactive interface to the contact layers [21, 22].

The optical absorption spectra of ZnO-Nrods and (ZnO-Nrod/P$_3$HT, ZnO-Nrod/PCPDTBT, and ZnO-Nrod/PTB7) thin films were confirmed, as shown in Figure 6 (inset). The absorption spectra of ZnO-Nrods correspond to the

Table 2: Effects of high light absorption polymers on the device' parameters such as short circuit current density (J_{sc}), open-circuit voltage (V_{oc}), fill factor (FF), and power conversion efficiency (η).

Polymers	V_{oc} (V)	J_{sc} (mA/cm^2)	FF (%)	η (%)
P3HT	0.6	10.26	36	2.25
PCBDTBT	0.5	12.62	35	2.54
PBT7	0.54	14.9	32	2.90

absorption band of 350–400 nm. The absorption spectra of ZnO/P$_3$HT thin films correspond to the absorption band region of 450–650 nm. Therefore, lower-band-gap energy polymers were designed to enhance the sunlight absorption. The absorption bands of the ZnO-Nrod/PCPDTBT and ZnO-Nrod/PTB7 correspond to the spectra region of 350–850 nm. In the BHJ solar cells, the polymer absorbs a narrow range of wavelengths in the visible spectrum. Since V_{oc} is determined by the energy gap between the

RMS ~ 4 nm RMS ~ 4.6 nm RMS ~ 4.9 nm RMS ~ 5.2 nm RMS ~ 5.5 nm

RMS ~ 5.8 nm RMS ~ 6 nm RMS ~ 6.7 nm RMS ~ 6.9 nm RMS ~ 7.2 nm
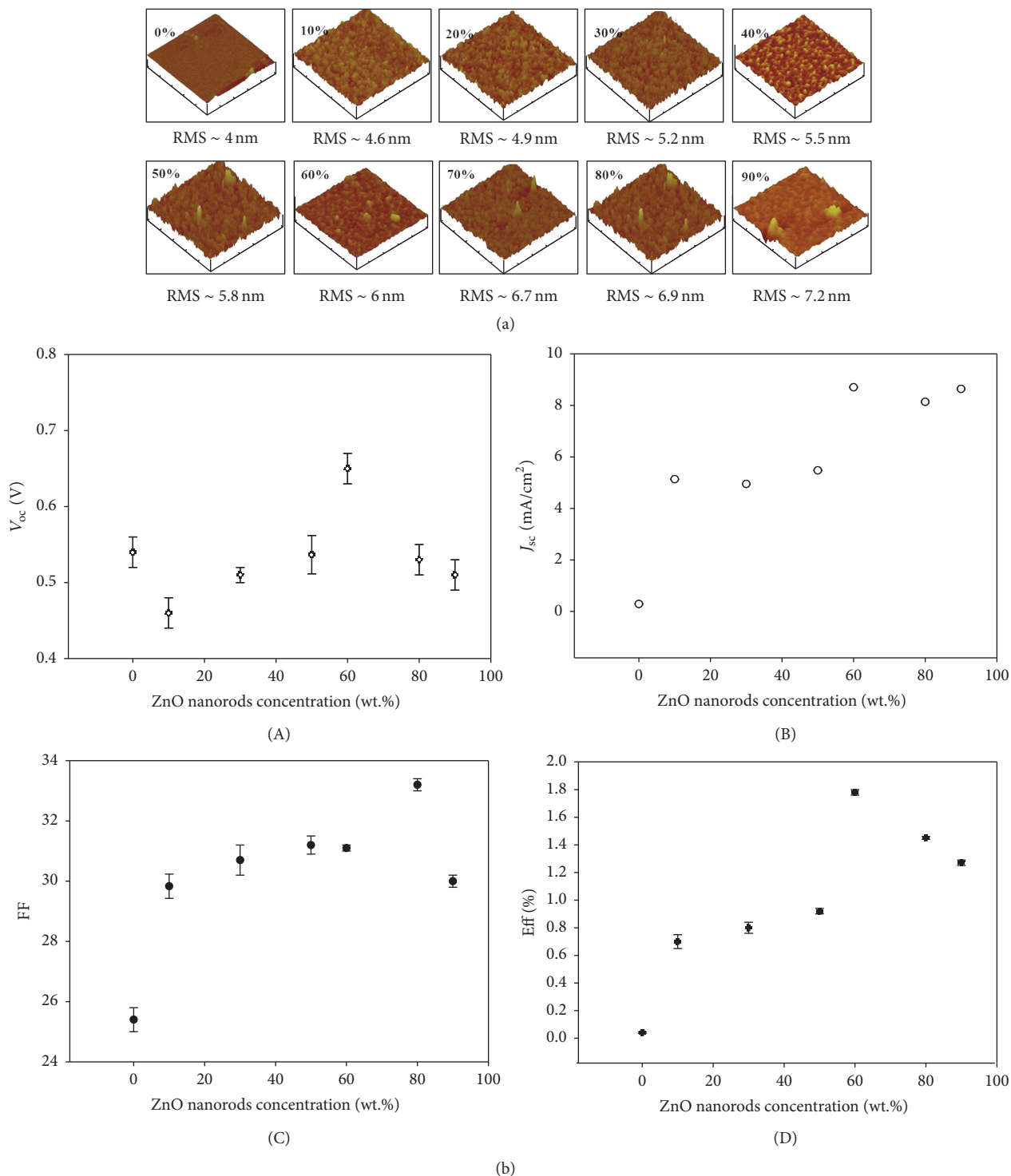
(a)

(A)

(B)

(C)

(D)

(b)

FIGURE 3: (a) Photoactive layer' surface morphology of solar cells with different composite loading amount of ZnO-Nrod/[ZnO-Nrod + P3HT] wt%. (b) Device's parameters with different composite loading amount of ZnO-Nrod/[ZnO-Nrod + P3HT] wt%.

donor HOMO and acceptor LUMO [23], the application of polymers with low band gaps as donors typically decreases V_{oc}, and a trade-off between light absorption and electrical properties is realized for both standard and inverted device geometries. Influences of the sunlight' harvesting on the device performance were studied. Table 2 shows that the open circuit voltage (V_{oc}) is slightly decreased from about ~0.6 to 0.5 eV when the lower-band-gap energy polymer was used, but the short circuit current density gradually increased.
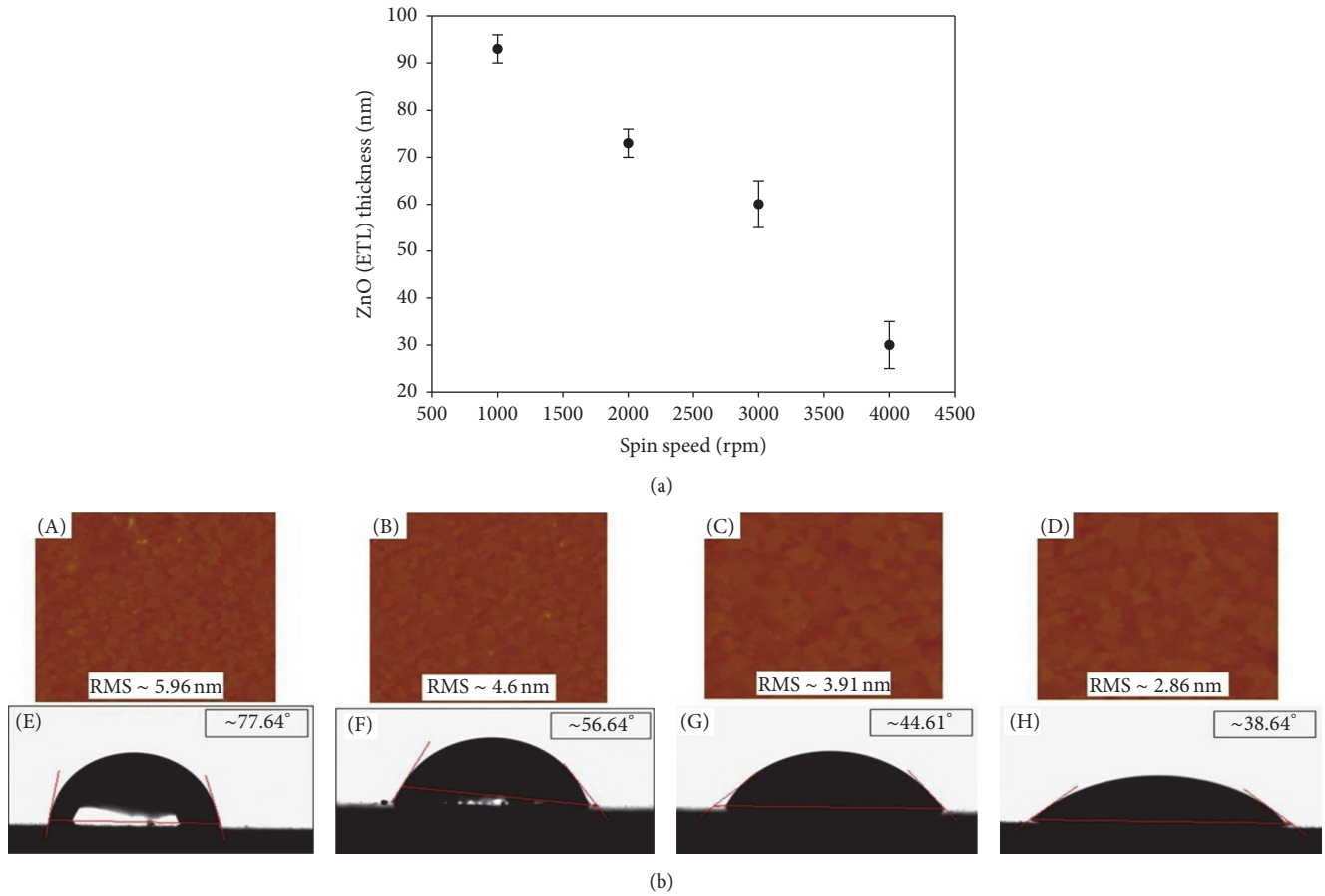
(a)

(b)

FIGURE 4: (a) The thickness and (b) surface roughness of electron transport layer (ETL) (ZnO nanoparticle) with a varying spin speed from 1000 to 4000 rounds per minute (rpm).
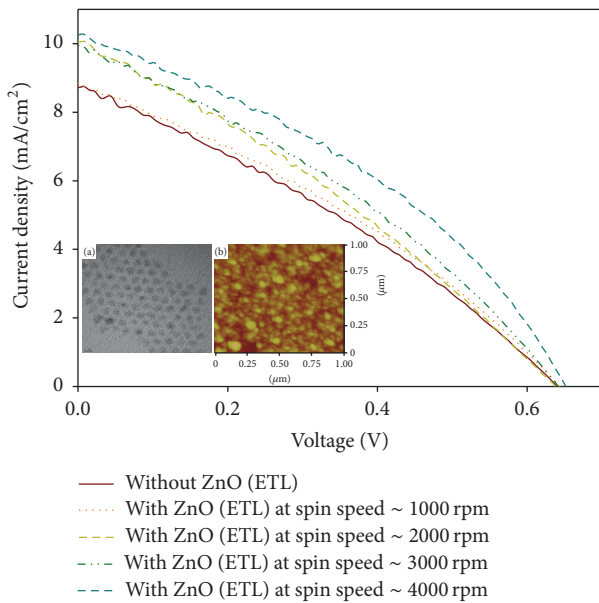

FIGURE 5: ((a), (b)) TEM image (inset) of ZnO nanoparticles and surface morphology of ZnO NPs/ITO film and J-V characteristic of device with and without electron transport layer as the junction of spin speed (round per minute).

Figure 6 shows the J-V curves of the ZnO-Nrods/ polymer devices; the efficiency of the devices was found to be enhanced from ~2.25% (J_{sc} ~ 10.26 mA/cm^2) of the ZnO/P3HT cell to ~2.54% (J_{sc} ~ 12.62 mA/cm^2) of the ZnO/PCPDTBT cell, with the maximum efficiency of about ~2.9% (J_{sc} ~ 14.9 mA/cm^2) of the ZnO/PTB7 cell. The enhanced efficiency was mainly due to the increase in the short circuit current from 10.26 to 14.9 mA/cm^2, which indicates an increase in the light absorption by PCPDTBT and PBT7 polymers, because the absorption wavelength is extended further within the visible region. Previous studies reported that the power conversion efficiency of the ZnO-Nrods solar cells was very low (~0.2 and ~0.9%), because the device fabrication process is not well optimized [24, 25]. p-type semiconductor ligand modification of ZnO nanorods is used to increase the device performance. The porphyrin and phthalocyamine molecules were incorporated at hybrid p-n junction interface; however, they found that adding of ligand modified ZnO-Nrods to the polymer leads to composite blends with poor photocurrent generation efficiency although the nanorods were highly dispersed inside the polymer. Zhong et al. [25] reported that they use Z907-modified ZnO nanorods and polymer, the effects of Z907 grafting on the light absorption, carriers transport, and
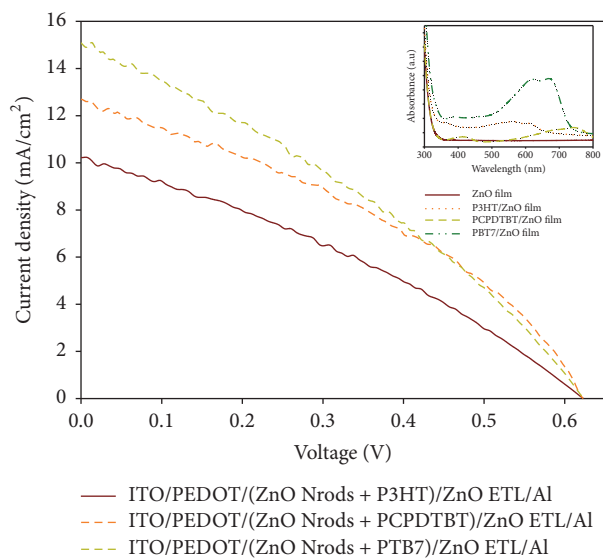
FIGURE 6: Absorption spectrum (inset) of ZnO-Nrod and (ZnO-Nrod + polymers) films and *J-V* characteristic of device with electron transport layer (ETL) and different low band gap energy polymers.

active layer surface morphology. But the device's conversion efficiency is still quite low in comparison with the previous inorganic hybrid solar cells (recorded efficiency of ~3%). Our cell performance with efficiency of ~2.9% is only compared to the recorded values reported for inorganic hybrid solar cells. Our device fabrication is quite different from previous reports and the efficiency of the cell with pure and random nanorods is bigger than ZnO NPs- and ligand modified ZnO nanorod/polymer cells.

4. Conclusions

In summary, we prepared high-performance inorganic BHJ solar cells with the addition of an electron transport layer (ZnO layer) by using a high-light-absorption polymer with low band gap energy, such as PCPDTBT and PTB7. We obtained power conversion efficiency as high as ~3% for the structure based on ZnO-Nrods and PTB7, by using a ZnO nanoparticle ETL. Therefore, this investigation opens new avenues for the structure design and development of electron transport materials for high-performance solar cells and many other optoelectronic devices.

Competing Interests

The authors declare that they have no competing interests.

Authors' Contributions

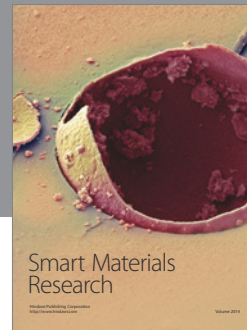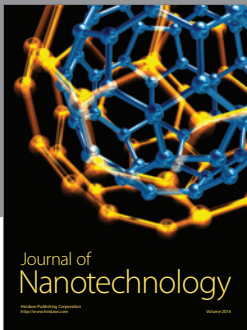Nguyen Tam Nguyen Truong and Hoa Nguyen contributed equally to this work.

References

[1] Y.-S. Cho and Y.-D. Huh, "Preparation and optical properties of green-emitting $BaMoO_4$:Tb^{3+},Na^+ nanophosphors for transparent displays," *Electronic Materials Letters*, vol. 10, no. 6, pp. 1185–1189, 2014.

[2] D. A. Van Den Ende, R. Hendriks, R. Cauchois, and W. A. Groen, "Large area photonic flash soldering of thin chips on flex foils for flexible electronic systems: in situ temperature measurements and thermal modelling," *Electronic Materials Letters*, vol. 10, no. 6, pp. 1175–1183, 2014.

[3] N. T. N. Truong and C. Park, "Enhancement of CdSe/Poly(3-hexylthiophene) bulk heterojunction solar cell efficiency by surface ligand exchange and thermal treatment," *Japanese Journal of Applied Physics*, vol. 51, no. 10, Article ID 10NE27, 2012.

[4] N. C. Greenham, X. Peng, and A. P. Alivisatos, "Charge separation and transport in conjugated-polymer/semiconductor-nanocrystal composites studied by photoluminescence quenching and photoconductivity," *Physical Review B*, vol. 54, no. 24, pp. 17628–17637, 1996.

[5] A. A. R. Watt, D. Blake, J. H. Warner et al., "Lead sulfide nanocrystal: conducting polymer solar cells," *Journal of Physics D: Applied Physics*, vol. 38, no. 12, pp. 2006–2012, 2005.

[6] W. U. Huynh, J. J. Dittmer, and A. P. Alivisatos, "Hybrid nanorod-polymer solar cells," *Science*, vol. 295, no. 5564, pp. 2425–2427, 2002.

[7] B. Sun, E. Marx, and N. C. Greenham, "Photovoltaic devices using blends of branched CdSe nanoparticles and conjugated polymers," *Nano Letters*, vol. 3, no. 7, pp. 961–963, 2003.

[8] B. O'Regan and M. Grätzel, "A low-cost, high-efficiency solar cell based on dye-sensitized colloidal TiO_2 films," *Nature*, vol. 353, no. 6346, pp. 737–740, 1991.

[9] S. A. Haque, S. Koops, N. Tokmoldin et al., "A multilayered polymer light-emitting diode using a nanocrystalline metal-oxide film as a charge-injection electrode," *Advanced Materials*, vol. 19, no. 5, pp. 683–687, 2007.

[10] R. Cinnsealach, G. Boschloo, S. N. Rao, and D. Fitzmaurice, "Electrochromic windows based on viologen-modified nanostructured TiO2 films," *Solar Energy Materials and Solar Cells*, vol. 55, no. 3, pp. 215–223, 1998.

[11] C. G. Granqvist, "Electrochromic tungsten oxide films: review of progress 1993–1998," *Solar Energy Materials and Solar Cells*, vol. 60, no. 3, pp. 201–262, 2000.

[12] Y.-M. Lee, C.-M. Huang, H.-W. Chen, and H.-W. Yang, "Low temperature solution-processed ZnO nanorod arrays with application to liquid ethanol sensors," *Sensors and Actuators, A: Physical*, vol. 189, pp. 307–312, 2013.

[13] L.-W. Ji, S.-M. Peng, J.-S. Wu, W.-S. Shih, C.-Z. Wu, and I.-T. Tang, "Effect of seed layer on the growth of well-aligned ZnO nanowires," *Journal of Physics and Chemistry of Solids*, vol. 70, no. 10, pp. 1359–1362, 2009.

[14] Z. H. Ibupoto, K. Khun, M. Eriksson et al., "Hydrothermal growth of vertically aligned ZnO nanorods using a biocomposite seed layer of ZnO nanoparticles," *Materials*, vol. 6, no. 8, pp. 3584–3597, 2013.

[15] W. J. E. Beek, M. M. Wienk, and R. A. J. Janssen, "Efficient hybrid solar cells from zinc oxide nanoparticles and a conjugated polymer," *Advanced Materials*, vol. 16, no. 12, pp. 1009–1013, 2004.

[16] W. J. E. Beek, M. M. Wienk, M. Kemerink, X. Yang, and R. A. J. Janssen, "Hybrid zinc oxide conjugated polymer bulk heterojunction solar cells," *Journal of Physical Chemistry B*, vol. 109, no. 19, pp. 9505–9516, 2005.

[17] D. C. Olson, S. E. Shaheen, R. T. Collins, and D. S. Ginley, "The effect of atmosphere and ZnO morphology on the performance of hybrid poly(3-hexylthiophene)/ZnO nanofiber photovoltaic devices," *Journal of Physical Chemistry C*, vol. 111, no. 44, pp. 16670–16678, 2007.

[18] I. Litzov and C. J. Brabec, "Development of efficient and stable inverted bulk heterojunction (BHJ) solar cells using different metal oxide interfaces," *Materials*, vol. 6, no. 12, pp. 5796–5820, 2013.

[19] M. A. Ibrahem, H.-Y. Wei, M.-H. Tsai, K.-C. Ho, J.-J. Shyue, and C. W. Chu, "Solution-processed zinc oxide nanoparticles as interlayer materials for inverted organic solar cells," *Solar Energy Materials and Solar Cells*, vol. 108, pp. 156–163, 2013.

[20] T. Hu, F. Li, K. Yuan, and Y. Chen, "Efficiency and air-stability improvement of flexible inverted polymer solar cells using ZnO/poly(ethylene glycol) hybrids as cathode buffer layers," *ACS Applied Materials and Interfaces*, vol. 5, no. 12, pp. 5763–5770, 2013.

[21] J. S. Bhat, A. S. Patil, N. Swami et al., "Electron irradiation effects on electrical and optical properties of sol-gel prepared ZnO films," *Journal of Applied Physics*, vol. 108, no. 4, Article ID 043513, 2010.

[22] M. Ohyama, H. Kozuka, and T. Yoko, "Sol–gel preparation of transparent and conductive aluminum-doped zinc oxide films with highly preferential crystal orientation," *Journal of the American Ceramic Society*, vol. 81, no. 6, pp. 1622–1632, 1998.

[23] C. Deibel and V. Dyakonov, "Polymer-fullerene bulk heterojunction solar cells," *Reports on Progress in Physics*, vol. 73, no. 9, Article ID 096401, 2010.

[24] S. Ben Dkhil, M. Gaceur, W. Dachraoui et al., "P-type semiconductor surfactant modified zinc oxide nanorods for hybrid bulk heterojunction solar cells," *Solar Energy Materials & Solar Cells*, vol. 159, pp. 608–616, 2017.

[25] M. Zhong, D. Sheng, C. Li, S. Xu, and X. Wei, "Hybrid bulk heterojunction solar cells based on poly (3-hexylthiophene) and Z907-modified ZnO nanorods," *Solar Energy Materials & Solar Cells*, vol. 121, pp. 22–27, 2014.

Journal of
Nanotechnology

International Journal of
Corrosion

International Journal of
Polymer Science

**Smart Materials
Research**

Journal of
Composites

**BioMed
Research International**

Journal of
Metallurgy

Journal of
Materials

Journal of
Nanoparticles

![Hindawi]
Submit your manuscripts at
https://www.hindawi.com

Advances in
Materials Science and Engineering

Scientifica

Journal of
Nanomaterials

**The Scientific
World Journal**

International Journal of
Biomaterials

Journal of
Nanoscience

Journal of
Coatings

Journal of
Crystallography

Journal of
Ceramics

Journal of
Textiles